Clim Dyn (2012) 39:919–928
DOI 10.1007/s00382-011-1232-9

Regional-scale winter-spring temperature variability and chilling damage dynamics over the past two centuries in southeastern China

Jianping Duan · Qi-Bin Zhang · Lixin Lv · Chao Zhang

Received: 20 April 2011 / Accepted: 24 October 2011 / Published online: 6 November 2011

Abstract Winter-spring cold extreme is a kind of serious natural disaster for southeastern China. As such events are recorded in discrete documents, long and continuous records are required to understand their characteristics and driving forces. Here we report a regional-scale winter-spring (January–April) temperature reconstruction based on a tree-ring network of pine trees (*Pinus massoniana*) from five sampling sites over a large spatial scale (25–29°N, 111–115°E) in southeastern China. The regional tree-ring chronology explains 48.6% of the instrumental temperature variance during the period 1957–2008. The reconstruction shows six relatively warm intervals (i.e., ~1849–1855, ~1871–1888, ~1909–1920, ~1939–1944, ~1958–1968, 1997–2007) and five cold intervals (i.e., ~1860–1870, ~1893–1908, ~1925–1934, ~1945–1957, ~1982–1996) during 1849–2008. The last decade and the 1930s were the warmest and coldest decades, respectively, in the past 160 years. The composite analysis of 500-hPa geopotential height fields reveals that distinctly different circulation patterns occurred in the instrumental and pre-instrumental periods. The winter-spring cold extremes in southeastern China are associated with Ural-High ridge pattern for the instrumental period (1957–2008), whereas the cold extremes in pre-instrumental period (1871–1956) are associated with North circulation pattern.

Keywords Tree rings · Regional temperature · Southeastern China · Chilling damage · Masson pine

J. Duan · Q.-B. Zhang (✉) · L. Lv · C. Zhang
State Key Laboratory of Vegetation and Environmental Change, Institute of Botany, Chinese Academy of Sciences, Beijing 100093, China
e-mail: qbzhang@ibcas.ac.cn

1 Introduction

In the course of global warming, regional low-temperature extremes also occurred intermittently and have drawn great attention to climate researchers as well as the public (Ding et al. 2008; Wen et al. 2009; Sun and Zhao 2010). An unusually cold January–February with heavy snow appeared in large areas of southeastern China in 2008. Such a severe cold condition, accompanied with strong wind, rain/snow and freezing temperature, occurred again in this region in January of 2011. These chilling events, usually lasting for a relatively long time and influencing an extensive area, not only influenced regional agriculture by reducing the production of crop, fruits and tea, but also caused dramatic damages in regional transportation and power infrastructure (Liu and Gao 2001; Zhao et al. 2008). Especially, our study area (Hunan and Jiangxi provinces) was a sensitive region of southern China that was influenced by winter-spring chilling damage/cold wave (Wen and Ding 2008; Liu and Gao 2001). It is therefore relevant to ask: (1) how often do these low-temperature extremes occur? and (2) which circulation pattern triggers the extremely cold events? The answers are of particular importance for southeastern China, which is a major center of China's agriculture and economic development with dense populations.

Using observed records from 1950s to 1990s, Liu and Gao (2001) reported that spring cold extremes occurred more often in the 1980s and less in the 1990s in southern China. Wei (2008) studied the winter-spring cold wave in 1955–2004 in China and pointed out that the frequency of cold wave decreased obviously since 1990s. Wang and Ding (2006) found that, during 1951–2003, the frequency of cold wave in China decreased gradually since the end of 1960s and reduced abruptly by the end of 1970s. The

results from these previous studies were limited by the length of the observed climate records. The regime of coldness occurrence in earlier time remains unknown.

The large-scale circulation patterns that might have triggered the cold waves in southern China were also studied previously based on observed climate records (Zhang et al. 2010; Kuang and Qin 2003; Gao et al. 2009; Gu et al. 2008). The results indicated that different circulation patterns/synoptic systems could induce cold waves in southern China. For example, based on the statistical analyses of synoptic course for the cold wave over 1959–1987, Wen and Chen (2006) summarized three possible circulation patterns including Ural-High ridge pattern, North circulation pattern and Trough-ridge circulation pattern that might have induced cold waves in Jiangxi province. The presence of different patterns indicated that the characteristics of the cold waves might differ from one cold extreme to the other. Therefore a better understanding of the circulation pattern for the cold extremes, especially during the historical period, requires a database larger than the observed record of coldness.

In this study, we attempted to extend the instrumental record of winter-spring temperature back to the last two centuries using tree rings as a proxy. Climate affects the growth of trees and the climate signal is recorded in the annual growth rings of the trees (Fritts 1976; Büntgen et al. 2005; D'Arrigo et al. 2005; Fang et al. 2010). Tree rings are well known for their accurate dating and high-resolution, and have played an important role in the reconstruction of winter and spring temperatures (Yadav and Singh 2002; Yonenobu and Eckstein 2006; Zhu et al. 2009; Shi et al. 2010). In southeastern China, Shi et al. (2010) studied tree-ring widths in the lower reaches of the Yangtze River and reported a winter temperature reconstruction for the period 1852–2006. The southeastern China is a large region covering a range of ~20–35°N and ~110–120°E and accounting for about ~1/4 of the total area of China. Thus, there is a need to enlarge tree-ring studies in the southeastern China.

The objectives of this study were (1) to reconstruct winter-spring temperature variations in the last two centuries for Hunan and Jiangxi provinces of southeastern China, (2) to examine the characteristics of cold extremes, and (3) to investigate the linkage of cold extremes to large-scale atmospheric circulation conditions. Our results are expected to better understand the characteristics of cold extremes in southeastern China on a longer time scale.

2 Data and methods

2.1 Tree-ring data

The study area is Hunan and Jiangxi provinces, southeastern China (Fig. 1). Tree-ring samples were collected from five sites of old growth Masson pine (*Pinus massoniana*) forest. Two sites were located in Hunan province and three sites were located in Jiangxi province (Fig. 1). At each site, increment core samples were collected from at least 30 old Masson pine trees. The elevation of the sampling sites ranged from 502 to 1431 m.a.s.l.

The ring width of each tree sample were processed, measured (to a precision of 0.001 mm) and crossdated following standard dendrochronological procedures (Fritts 1976; Cook and Kairiukstis 1990). Samples that cannot be crossdated due to poor quality (such as containing too many rotten or broken pieces) were removed from further analyses. A total of 144 samples were successfully crossdated and the lowest number of samples within a site is 24 samples. At each site, a tree-ring width standard chronology was developed using the program ARSTAN (Cook 1985), in which a cubic smoothing spline with 50% frequency–response cutoff equal to 80 years was employed to remove non-climatic, tree-age related growth trends. Since the five site-chronologies significantly correlate to each other (mean $r = 0.338$, $p < 0.001$, n = 109, for the common period 1900–2008) and the mean inter-series correlation coefficient of all the 144 samples is $r = 0.346$ for a window of 50 years, a regional chronology was developed using all the 144 samples. When anomalous growth trends occurred within a sample, the length of the detrending spline was adjusted to 40 years (15 samples were adjusted). Compared with other detrending methods (i.e., negative exponential curve and linear regression curve), such detrending method could retain the common signals among individual tree-ring series while removing noise from

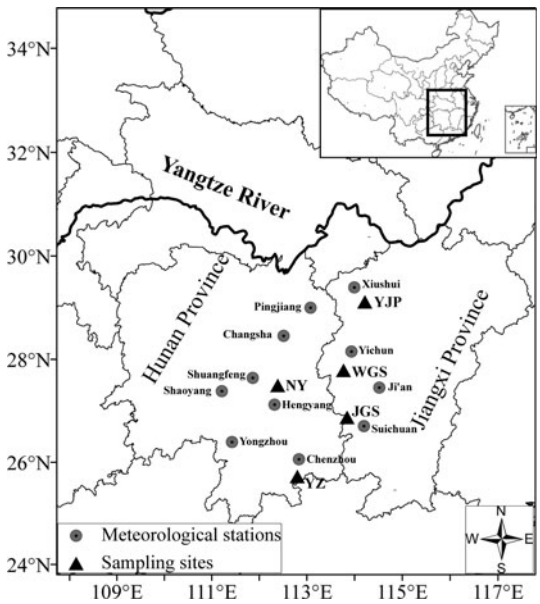

Fig. 1 Map showing the locations of the five tree-ring sampling sites and eleven meteorological stations

Table 1 Site characteristics about the five sampling sites and statistics of standard chronologies

Sites	Latitude/longitude	Elevation	Time-span	Species	Trees	R_{bt}	MS	SD	AC1
YJP	28°44′N/114°47′E	941 m	1858–2008	*Pinus massoniana*	32	0.326	0.181	0.195	0.324
WGS	27°27′N/114°10′E	1431 m	1835–2008	*Pinus massoniana*	24	0.520	0.151	0.183	0.517
NY	27°16′N/112°42′E	603 m	1818–2008	*Pinus massoniana*	33	0.292	0.220	0.243	0.291
JGS	26°32′N/114°09′E	866 m	1806–2008	*Pinus massoniana*	26	0.477	0.193	0.225	0.474
YZ	25°28′N/112°58′E	502 m	1819–2008	*Pinus massoniana*	29	0.427	0.165	0.213	0.425
RC	–	–	1806–2008	*Pinus massoniana*	144	0.336	0.134	0.155	0.334

RC regional tree-ring width standard chronology composed of the five sampling sites, R_{bt} correlation coefficient between trees, *MS* mean sensitivity, *SD* standard deviation, *AC1* first order autocorrelation

possible non-climate factors. Site characteristics of the five sampling sites and statistics of the chronologies are listed in Table 1.

As the sample size generally declines in the early portion of a tree-ring chronology, the subsample signal strength (SSS) was used to evaluate the most reliable time span of chronology (Wigley et al. 1984). To ensure the reliability of the regional chronology, it was truncated at the year when the value of SSS became smaller than 0.80.

2.2 Climate data

Climate data from 11 meteorological stations around the five sampling sites were used to generate the regional climate data (Fig. 1). The common period of these climate data was 1957–2008. Four climatic variables, i.e., monthly mean, minimum, and maximum temperature and monthly total precipitation, are of particular interest in this study. To ensure homogeneity of the climate from the 11 meteorological stations, correlation analyses and homogeneity test were performed using the DPL-HOM program (Holmes 1994). The correlation coefficients of January–April mean temperature, minimum temperature, maximum temperature and precipitation among the 11 stations during 1957–2008 range from 0.850 to 0.992 ($p < 0.0001$), 0.830–0.988 ($p < 0.0001$), 0.805–0.969 ($p < 0.0001$) and 0.245–0.881 ($p < 0.1$), respectively. The results show that the three temperature variables are more homogeneous than precipitation though they are all quite homogeneous. Therefore, the regional data averaged from the 11 meteorological stations were used to represent the regional climate of the study area.

According to the regional meteorological data during the period 1957–2008, mean annual temperature is 17.6°C, and annual precipitation is around 1149.0 mm. Mean maximum monthly temperature is 29.0°C in July, and mean minimum monthly temperature is 5.5°C in January (Fig. 2). The geopotential height data obtained from the NOAA/OAR/ESRL PSD (http://www.esrl.noaa.gov/psd/) have a spatial resolution of 2° latitude by 2° longitude and cover the period 1871–2008.

2.3 Methods

Relationships between tree-ring growth and climate factors were identified via the correlation analysis from 1957 to 2008. Spatial field correlation analysis was used to examine the spatial scope of the relationship between the tree-ring chronology and climate data from CRUts 3 dataset (Mitchell and Jones 2005).

Past climate was reconstructed from tree rings using linear regression analysis. The skill of the regression model was verified using split-sample method (Meko and Graybill 1995). The statistics for evaluation of the regression model include Pearson's correlation coefficient (r), sign test (ST), first difference sign test (ST1), reduction of error (RE), and coefficient of efficiency (CE). Both RE and CE are measures of shared variance between actual and estimated series (CE is a more rigorous verification statistic), with a positive value suggesting that the reconstruction has encouraging performance (Cook et al. 1994).

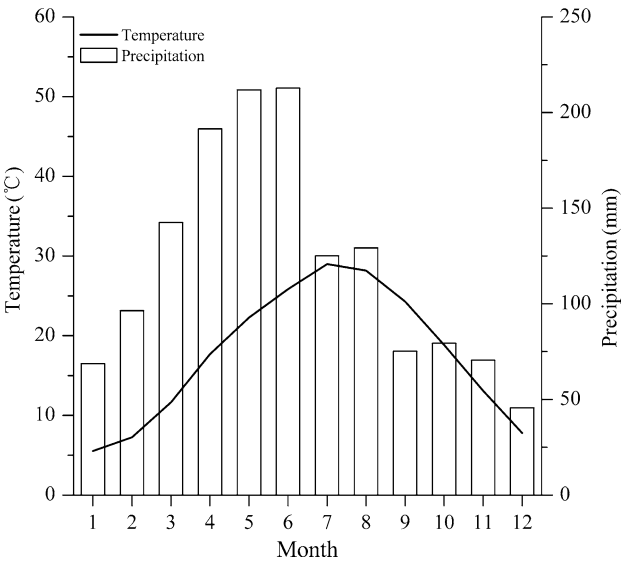

Fig. 2 Monthly mean temperature and total precipitation averaged from eleven meteorological stations in the study region during 1957–2008

The 500-hPa geopotential height fields in years of extreme January–April temperatures were examined by composite analysis. During 1871–2008, the anomalous cold years (temperature <mean $-\ \sigma$) and anomalous warm years (temperature >mean $+\ \sigma$) were defined. The contours of the composite geopotential height were calculated as the difference between the mean of 500-hPa geopotential heights in anomalous cold years and the mean of 500-hPa geopotential heights in anomalous warm years (the mean of cold years minus the mean of warm years). The geopotential height field for single year with extreme January–April temperature was also examined.

3 Results

3.1 Regional tree-ring width chronology

The regional tree-ring width standard chronology (RC) established with 144 trees covers a 203-year length, starting from 1806 and ending in 2008. The threshold of SSS >0.80 corresponds to a minimum sample depth of 15 trees back to year 1849, and SSS >0.85 corresponds to 17 trees back to year 1851 (Fig. 3).

3.2 Relationships between tree-ring growth and climate

The correlation pattern between regional chronology and monthly mean, maximum, and minimum temperature are similar (Fig. 4). At the $p < 0.05$ level of significance, tree rings are positively correlated with temperature in January, February and March, and with precipitation in April. The highest correlation is found in the January–April mean temperature ($r = 0.697$, n = 52, $p < 0.0001$).

3.3 Reconstruction of January–April temperature

Based on the growth-climate response relationship, January–April mean temperature was reconstructed. A linear regression model was established using the January–April mean temperature as the dependent variable and the regional chronology as the independent variable.

The statistics in the verification and calibration are significant at the level of $p < 0.01$, except for the ST and ST1 values for the verification sub-period of 1983–2008 ($p < 0.25$) (Table 2). The values of the two most rigorous tests for model validation, the reduction of error (RE) and the coefficient of efficiency (CE) were positive for both verification intervals indicating good performance of the regression model (Fritts 1976; Cook and Kairiukstis 1990).

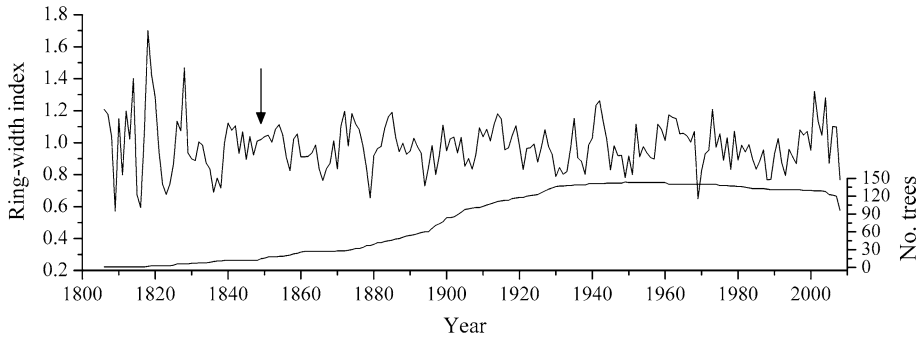

Fig. 3 Regional tree-ring width standard chronology of *Pinus masson* and the sample replication. *Arrow* denotes the year with SSS >0.8

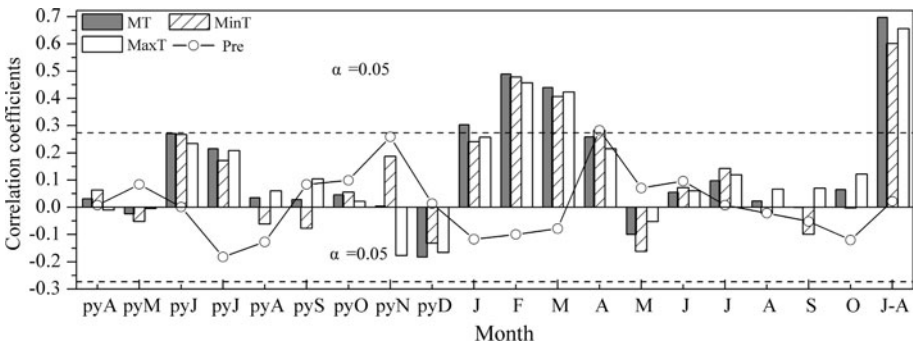

Fig. 4 Correlation coefficients between the regional ring-width standard chronology and temperature and precipitation (averaged from eleven meteorological stations) from previous April to current October and January–April means over the period 1957–2008. MT, MinT, MaxT and Pre represent monthly mean temperature, minimum temperature, maximum temperature and monthly precipitation, respectively; "py" means previous year, J–A means January to April; horizontal dotted lines indicate statistical significance level of 0.05

Table 2 Statistics of the sub-period calibration and verification of reconstruction model

Calibration					Verification					
Period	*r*	R^2	R^2_{adj}	F	Period	*r*	RE	ST	ST1	CE
1957–1982	0.71[a]	0.504	0.483	24.4[a]	1983–2008	0.732[a]	0.425	17/9	16/9	0.354
1983–2008	0.736[a]	0.536	0.516	27.7[a]	1957–1982	0.71[a]	0.33	21/5[a]	20/5[a]	0.192
1957–2008	0.697[a]	0.486	0.476	47.3[a]						

ST sign test, *ST1* first difference sign test, *RE* reduction error, *CE* coefficient of efficiency. The [a] indicate the significance level of 0.01

Therefore we developed the final transfer function using the actual January-April temperature (T_{1-4}) and the regional chronology (RC) over the common period 1957–2008.

$$T_{1-4} = 5.956 + 4.608 \times RC$$

The regional chronology in the transfer function explains 48.6% ($R^2_{adj} = 47.6\%$) of the total variance in January–April temperature in the period 1957–2008. The temperature series derived from the model agrees well with the actual temperature series (Fig. 5). January–April mean temperature for the past 160 years (A.D. 1849–2008) could thus be reconstructed by applying the regional tree-ring chronology to the regression model (Fig. 6).

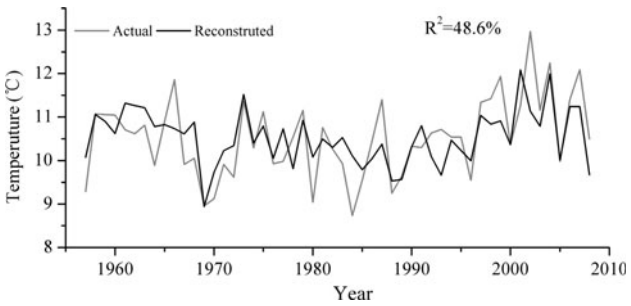

Fig. 5 Comparison of actual and reconstructed January–April mean temperature in the period 1957–2008 for the southeastern China

The years of climatic extremes were identified by examining the reconstructed January–April temperature values that exceed one standard deviation ($\sigma = \pm 0.562$°C). The temperature reconstruction showed 27 anomalous warm years (greater than one standard deviation) and 28 anomalous cold years (smaller than minus one standard deviation) in the past 160 years, each accounting for about ~17% of the total years (Fig. 6).

The decadal temperature departure relative to the whole time span (1849–2008) and the number of anomalous warm and cold years for every 10 years were calculated (Table 3). The highest positive temperature departure (0.49°C) occurred in the last decade and the highest negative temperature departure (−0.39°C) occurred in the 1930s. There are five anomalous warm years in the last decade and five anomalous cold years in the 1930s. These are the two decades that extremely warm and cold years occurred most frequently in the past 160 years.

A 10-year FFT (Fast Fourier Transform) smoothing curve of the reconstruction shows relatively warm intervals during ~1849–1855, ~1871–1888, ~1909–1920, ~1939–1944, ~1958–1968 and 1997–2007. In contrast, cold intervals occurred during ~1860–1870, ~1893–1908, ~1925–1934, ~1945–1957 and ~1982–1996 (Fig. 6).

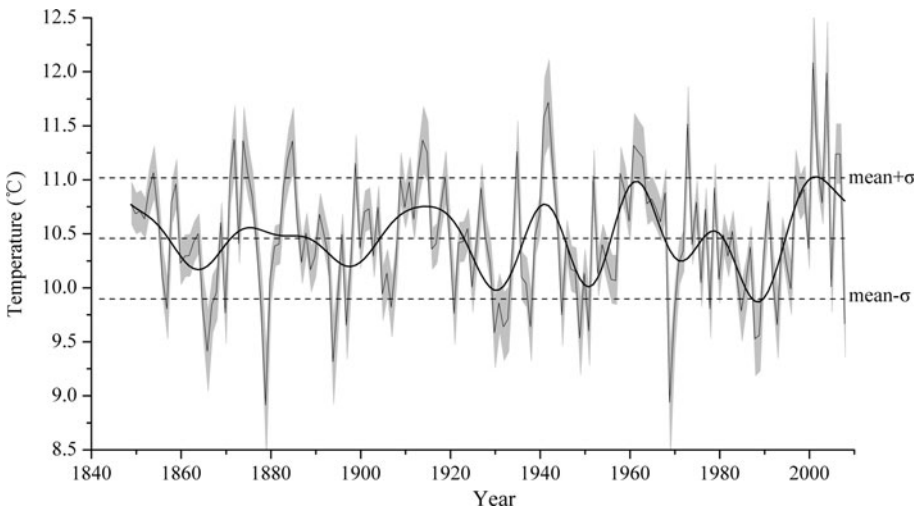

Fig. 6 Regional-scale January–April temperature variability reconstructed from tree rings in southeastern China. Superimposed on the reconstruction is the 10-year smoothing average. *Dash lines* are mean ± σ and shade area is the 95% confidence interval

Table 3 Mean temperature departure and the number of anomalous cold and warm years at every 10 years

Period	TD	No. C	No. W	Period	TD	No. C	No. W
1849–1859	0.19	1	1	1940–1949	0.12	2	3
1860–1869	−0.32	3	0	1950–1959	−0.09	1	2
1870–1879	0.04	3	3	1960–1969	0.26	1	3
1880–1889	0.13	0	2	1970–1979	0	2	1
1890–1899	−0.21	3	1	1980–1989	−0.38	3	0
1900–1909	−0.06	1	0	1990–1999	−0.03	1	1
1910–1919	0.4	0	4	1999–2008	0.49	1	5
1920–1929	−0.09	1	0	1849–2008	0	28	27
1930–1939	−0.39	5	1				

TD temperature departure, *No. C* number of cold years, *No. W* number of warm years

3.4 Circulation patterns in the years with extreme January–April temperature

Composite analysis of the 500-hPa geopotential height fields in the years of extreme January–April temperature (Fig. 6) reveals that, in the instrumental period 1957–2008, cold conditions were associated with a distinct high-pressure ridge located near the Ural Mountain (30°–60°E) and accompanied with a clear horizontal trough in front of it (Fig. 7a). Such pattern was quite similar for both instrumental data and tree-ring data. When using tree-ring data to examine the circulation pattern in the pre-instrumental period 1871–1956, the composite analysis shows a strong and wide High ridge (50°–110°E) with a very weak horizontal trough in its front (Fig. 7b). For the two coldest winter-spring years over the past 160 years in southeastern China, i.e., years 1879 and 1969, different circulation structures were found (Fig. 7c, d). A polar vortex was obvious in 1879, while an eastern Asian trough was dominant in 1969.

4 Discussion

4.1 Signal of January–April temperature in tree rings

The growth-climate response relationship (Fig. 4) suggests that the tree-ring width of Masson pine is a useful indicator of winter-spring temperature in southeastern China. Decreased winter-spring temperature might increase chilling damage to roots and delay the beginning of radial growth (Zhu et al. 2009; Shi et al. 2010). Similar growth-response relationship was also reported for Taiwan pine (*Pinus taiwanensis*) in the lower reaches of the Yangtze River (Shi et al. 2010), Korean Pine (*P. koraiensis*) in Changbai Mountain (Zhu et al. 2009), Hinoki cypress (*Chamaecyparis obtusa*) in central Japan (Yonenobu and Eckstein 2006), dragon spruce (*Picea balfouriana*) in west Sichuan plateau (Shao and Fan 1999), six tree species in the Hudson River Valley (Pederson et al. 2004), Qilian juniper (*Sabina przewalskii Kom.*) and Qinghai spruce (*Picea crassifolia Kom.*) on the northeast Tibetan Plateau (Liang et al. 2006; Zhu et al. 2008), Juniper trees

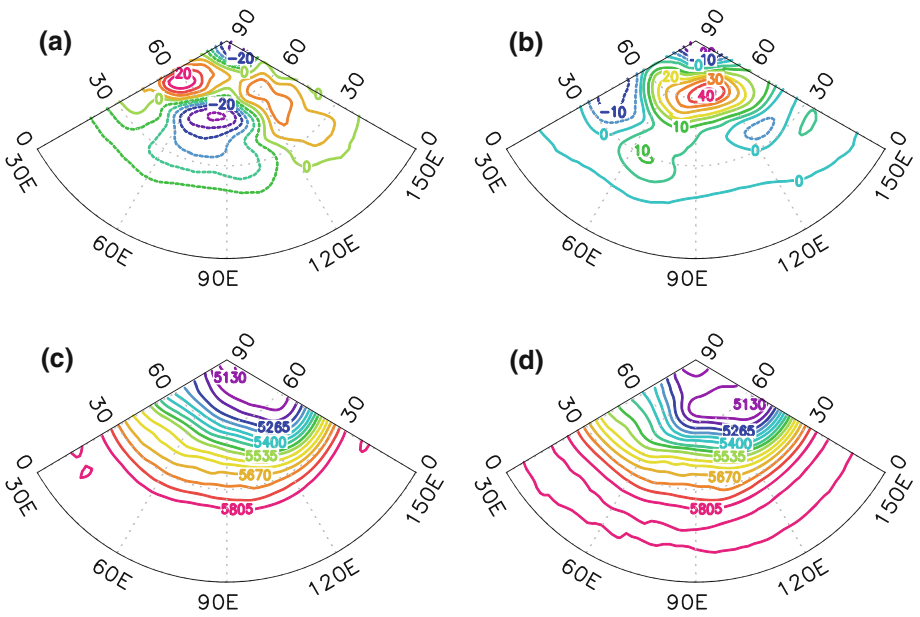

Fig. 7 Composite January–April 500 hPa geopotential height (gpm) of instrumental period (1957–2008) (**a**) and pre-instrumental period (1871–1956) (**b**), and the single-year January–April 500 hPa geopotential height (gpm) for year 1879 (**c**) and year 1969 (**d**)

(*Juniperus przewalskii*) in the Xiqing Mountains of the northeastern Tibetan Plateau (Gou et al. 2007) and Chinese pine (*Pinus tabulaeformis*) in the southern Qinling Mountains (Liu et al. 2009). These results indicated that winter-spring temperature plays an important role in the growth of tree-ring widths.

The regional tree-ring width chronology (RC) was significantly correlated with January–April surface temperature over a large area in southeastern China, and the highest correlation occurred in our study region ($r > 0.6$, $n = 50$) (Fig. 8). This observation indicates that our tree-ring chronology could well represent the regional-scale January–April temperature variability.

We also found that the signal of January–April temperature is stronger in the regional chronology than that in any individual site chronology. The correlation coefficient between any individual site ring-width standard chronology and January-April temperature of the nearest meteorological station ranges from 0.43 to 0.56 (for years 1957–2008), whereas the correlation coefficient is 0.697 ($n = 52$, for years 1957–2008) between the regional ring-width standard chronology and the regional January–April temperature. These suggest that the tree rings in southeastern China contained large-scale climatic signals yet these signals in tree rings were diluted at single sites. Therefore a tree-ring network is required for large-scale climate reconstruction in southeastern China.

4.2 Linkages between the frequency of climatic extremes and climate change

Our regional tree-ring chronology has well reflected the January–April temperature variation in southeastern China. In particular, it provides valuable information about winter-spring cold extremes occurred in southeastern China. Such information could be validated by historical documentations. The nine coldest years in the tree-ring reconstruction were all recorded in documents as prevailing coldness with a large spatial extent (Table 4). Non-disastrous warm winter-spring seasons were documented rarely. Only one (i.e., year 1914) of the six extremely warm years before instrumental record was validated by phenological record (Fang et al. 2005).

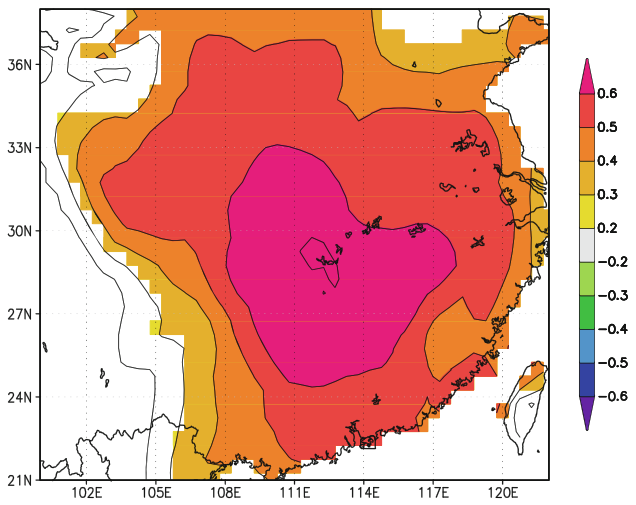

Fig. 8 Correlation field of the regional tree-ring indices with gridded January–April temperature during 1957–2006. The analysis was performed using the KNMI climate explorer (http://climexp.knmi.nl), the gridded climate dataset (CRUts3; Mitchell and Jones 2005) was available online

The distinctly reduced frequency of winter-spring cold extremes since 1990s (Table 3) was in agreement with the studies on cold wave events during the instrumental period in China (Wei 2008; Liu and Gao 2001; Wang and Ding 2006), suggesting a result of large-scale warming in China (Wei 2008; Wang and Ding 2006). The relatively more frequent cold extremes in the 1980s were only reported in southern China (Liu and Gao 2001). The frequency of cold extremes in the 1950s, 1960s and 1970s was less than that in the 1980s, an observation in agreement with the studies in southern China (Liu and Gao 2001). The frequency of cold extremes in pre-instrumental period was compared with the winter (December–March) temperature reconstruction in the lower reaches of the Yangtze River in southeastern China (Shi et al. 2010) and the spring (February–April) temperature variation in northeastern China (Zhu et al. 2009) (Fig. 9). Our reconstruction correlates well with the December-March temperature reconstruction in the lower reaches of the Yangtze River (Shi et al. 2010) in the cold epochs of ~1925–1934, ~1945–1957 and ~1982–1996, respectively, indicating that more frequent winter-spring extreme cold years occurred in these periods in southern China. Two obviously cold periods, 1900–1910 and 1860–1870, were shown in our study but absent in the lower reaches of the Yangtze River. The cold period of 1860s–1870s was not found in other studies of eastern China either. The cold period 1900–1910 was documented in the phenological records in Changsha and Hengyang in our studied region (Fang et al. 2005). Thus the two early periods with more frequent extreme cold years might occur only in our studied region. The comparison suggests that the frequent cold extremes in some periods were caused by regional climate change.

From a large-scale perspective, general disagreement for the winter-spring temperature variation was found between southeastern (Fig. 9b, c) and northeastern China (Fig. 9a). However, the two regions had a similar cold period in the 1930s and a warming trend since the 1990s (Fig. 9). These two periods just were the coldest and the warmest periods and had the most cold and warm extremes in the past 160 years, respectively. This implies that large-scale dramatic temperature change contributes to the more frequent occurrence of climatic extreme years. Overall, we found that winter-spring cold extremes in southeastern China were mainly induced by regional climate variation, and

Table 4 The 9 coldest years (temperature $<-1.5\sigma$) and 10 warmest years (temperature $>1.5\sigma$) based on January–April temperature reconstruction (1849–2008) and comparison with documented evidence of prevailing climate condition or related cold wave/chilling damage events

Year	Temperature anomaly	Description of climatic condition in historical documents
Cold spells		
1879	−1.54	*Jiangxi*: heavy rain with hail in March, spoiling seeding
1969	−1.52	*National*: cold wave in January, February and April, many regions presented the lowest temperature over the past ten years, a lot of crops, fruit trees and livestock were frozen to death; *Hunan*: air temperature dropped to −18.1°C on January 31, the lowest value within instrumental records (1951–1969); *Jiangxi*: 49 rainy days persisted (February 15–April 4) with low temperature; the regional January–April temperature departure is −1.57°C relative to the mean of 1957–2008
1894	−1.14	*Hunan*: heavy hail in Daoxian, Zhijiang and other near regions in April, houses and corps were severely damaged, some people and livestock were died
1866	−1.04	*Jiangxi*: heavy rain in spring, heavy snow and hail in January, freezing lasted for more than forty days
1988	−0.928	*Jiangxi*: strong cold wave in March, sixty-three counties suffered a 8–9 grade strong wind, twelve counties suffered hail with many winter corps, fishing boats damaged and people died; The regional January–April temperature departure is −1.28 relative to the mean of 1957–2008
1949	−0.92	*Jiangxi*: heavy rain in Mar–Apr, severe flood damage; *Hunan*: persisting rainy days in Spring-Summer and with strong wind
1989	−0.896	*Jiangxi, Hunan and Hubei*: strong cold air current from the north in Jan and Feb, heavy snow, low temperature and serious freezing disaster; freezing and cold damage in the central south and southwestern China; regional Jan–Apr temperature departure is −0.88°C compared to the mean of 1957–2008
1930	−0.873	*Hunan*: seldom coldness in Jan–Feb in the past 40 years; *Jiangxi*: snow cover more than forty days, many livestock were frozen to death; *Guangdong*: cold wave in January
1951	−0.855	*Hunan*: large-area cold spell in late spring
Warm spells		
2001	1.62	Jan–Apr temperature anomaly is 0.74°C with respect to the mean of 1957–2008
2004	1.53	Jan–Apr temperature anomaly is 1.72°C
1942	1.26	–
1941	1.12	–
1973	1.06	Jan-Apr temperature anomaly is 0.84°C
1872	0.92	–
1914	0.91	*Hunan*: The phenophase of Changsha and Hengyang in spring was 9 days earlier than the present day
1874	0.906	–
1885	0.9	–
1961	0.86	Jan-Apr temperature anomaly is 0.18°C

dramatic large-scale temperature change could lead to anomalously frequent winter-spring temperature extremes.

4.3 Different circulation patterns in instrumental and pre-instrumental periods

The active period for the outbreak of winter-spring cold wave in southwestern China mainly occurred in January–April (Zhang et al. 2010). Examination of the 500-hPa geopotential height fields via composite analyses of our reconstruction indicates that the circulation patterns in the years with extreme January–April temperatures differed at and before instrumental period.

In the instrumental period (1957–2008), the circulation pattern associated with cold extremes was similar to the Ural-High ridge pattern which referred to a strong NE-SW High ridge located near the Ural Mountain (30°–60° E) and usually accompanied with a blocking High. There was a clear horizontal trough in the east of Ural, when the horizontal trough was destroyed and a cold wave intruded into Jiangxi province (Wen and Chen 2006).

In the pre-instrumental period (1871–1956), the circulation pattern associated with cold extremes was similar to the North circulation pattern which referred to a strong and wide High ridge (50°–110°E) with a weak horizontal trough in its front. When the horizontal trough turned to longitudinal, a cold wave intruded into southeastern China, and the strength of the cold air under this pattern was very strong (Wen and Chen 2006). The results suggested that the driving forces for the occurrence of extreme coldness were different through time.

Examination of the 500-hPa geopotential height fields for single extreme cold years also suggests that different circulation structures occurred in different cold extremes.

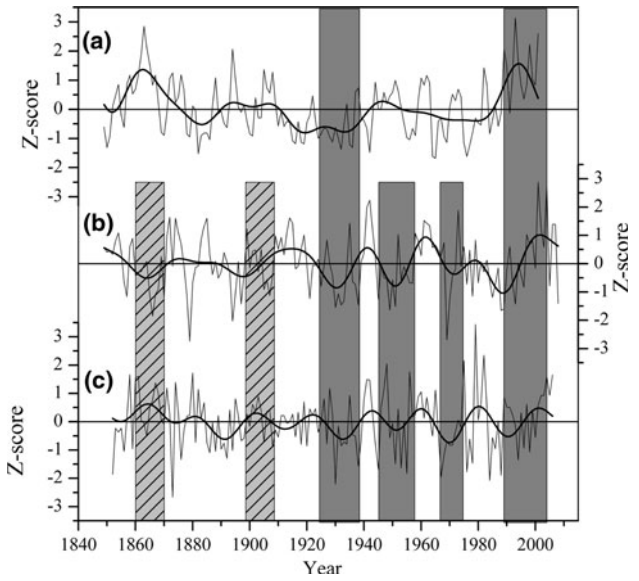

Fig. 9 Comparison of January–April temperature reconstructed in this study (*b*) with February–April temperature reconstruction for Changbai Mountain in Northeast China (*a*) and previous December to current March temperature reconstruction in the lower reaches of the Yangtze River (*c*)

The year 1879 was the coldest in January–April temperature over the past 160 years, and heavy rain and hail were also documented in this year for southeastern China (Table 4). The Polar vortex was a main synoptic system triggering this winter cold event in China, and it is a symbol for the large-scale extreme cold air (Zhu et al. 2000). Cold waves triggered by polar vortex were also reported in Guangxi province (south of our study area) Kuang and Qin 2003. Yi et al. (2009) pointed out that the strong stratospheric polar vortex had important influence on the snow calamity in southern China in January–February of 2008. Differently, the second coldest winter-spring in year 1969 mainly originated from the East Asian trough, which was also reported in Guizhou that locates more western to our studied area (Zhang et al. 2010). Historical records of climate conditions for the winter-spring in 1969 documented that national cold wave occurred in China in January, February and April, and many regions showed the lowest temperature in that year among the previous ten years (Table 4). Our long-period record of coldness is helpful for better understanding the circulation patterns that have triggered the extreme winter-spring coldness in southeastern China in different historical periods.

5 Conclusions

Our study found that the tree-ring width of Masson pine is a useful indicator of winter-spring temperature in southeastern China. The site tree-ring chronologies of Masson pine correlates significantly with January–April temperature, however such correlation is stronger in the regional chronology than that at any individual site chronology. Thus we conclude that a tree-ring network is essential for the large-scale climate reconstruction in southeastern China.

Based on the regional tree-ring width standard chronology, the January–April temperature at regional-scale (25–29°N, 111–115°E) was reconstructed back to year 1849. The results show that relatively warm intervals occurred during ~1849–1855, ~1871–1888, ~1909–1920, ~1939–1944, ~1958–1968 and 1997–2007, and cold intervals occurred during ~1860–1870, ~1893–1908, ~1925–1934, ~1945–1957 and ~1982–1996, respectively. In the past 160 years, the highest positive temperature departure (0.49°C) happened in the last decade and the highest negative temperature departure (−0.39°C) occurred in the 1930s. There are five anomalous warm years over the last decade and five anomalous cold years in the 1930s. These are the two decades that extremely warm and cold year occurred most frequently over the past 160 years. Documental evidences validated the signal of winter-spring cold extremes embedded in the regional tree-ring chronology in southeastern China.

Different circulation patterns could be present for different cold extremes and different periods. Dominant polar vortex triggered the coldest January–April of 1879 over the past 160 years, while the East Asian trough was responsible for the second coldest winter-spring coldness in 1969. In the instrumental period, the Ural-High ridge pattern was obvious, while the North circulation pattern was dominant in pre-instrumental period.

Acknowledgments This study was supported by the National Natural Science Foundation Projects No. 40631002 and No. 40890051. We are grateful to Dr. Zhu HF and Dr. Shi JF for making their original reconstructions available. Climate data from the meteorological stations were obtained from the National Meteorological Information Center of China Meteorological Administration.

References

Büntgen U, Esper J, Frank DC, Nicolussi K, Schmidhalter M (2005) A 1052-year tree-ring proxy for Alpine summer temperatures. Clim Dyn 25:141–153

Cook ER (1985) A time series analysis approach to tree-ring standardization. PhD Thesis, University of Arizona, Tucson

Cook ER, Kairiukstis LA (1990) Methods of dendrochronology. Kluwer, Netherlands

Cook ER, Briffa KR, Jones PD (1994) Spatial regression methods in dendroclimatology: a review and comparison of two techniques. Int J Climatol 14:379–402

D'Arrigo R, Mashig E, Frank D, Wilson R, Jacoby G (2005) Temperature variability over the past millennium inferred from Northwestern Alaska tree rings. Clim Dyn 24:227–236

Ding YH, Wang ZY, Song YF, Zhang J (2008) The unprecedented freezing disaster in January 2008 in southern China and its

possible association with the global warming. Acta Meteor Sin 22:538–558

Fang XQ, Xiao LB, Ge QS, Zheng JY (2005) Change of plants phenophases and temperature in spring during 1888–1916 around Changsha and Hengyang in Hunan province (in Chinese with English abstract). Quat Sci 25:74–79

Fang KY, Gou XH, Chen FH, Li JB, D'Arrigo R, Cook ER, Yang T, Davi N (2010) Reconstructed droughts for the southeastern Tibetan Plateau over the past 568 years and its linkages to the Pacific and Atlantic Ocean climate variability. Clim Dyn 35:577–585

Fritts HC (1976) Tree rings and climate. Academic Press, London

Gao AN, Chen J, Li SY, He DY, Huang MC, Luo JY (2009) Causation analysis of a rare chilling damage in the west of Soutch China in 2008 (in Chinese with English abstract). J Trop Meteorol 25:100–116

Gou XH, Chen FH, Jacoby G, Cook ER, Yang MX, Peng JF, Zhang Y (2007) Rapid tree growth with respect to the last 400 years in response to climate warming, northeastern Tibetan Plateau. Int J Climatol 27:1497–1503

Gu L, Wei K, Huang RH (2008) Severe disaster of blizzard, freezing rain and low temperature in January 2008 in China and its association with the anomalies of east Asian monsoon system (in Chinese with English abstract). Clim Environ Res 13:405–418

Holmes RL (1994) Dendrochronology program library (Diskette). Laboratory of Tree-Ring Research, University of Arizona, Tucson

Kuang XY, Qin ZN (2003) Statistical characteristics of cold wave weather in Guangxi and analysis of circumfluence Situation (in Chinese with English abstract). J Guangxi Meteorol 24:40–45

Liang EY, Shao XM, Eckstein D, Huang L, Liu XH (2006) Topography- and species-dependent growth responses of *Sabina przewalskii* and *Picea crassifolia* to climate on the northeast Tibetan Plateau. For Ecol Manag 236:268–277

Liu CF, Gao B (2001) Climate of chilling damage in spring in southern China and its atmospheric circulation features (in Chinese with English abstract). J Trop Meteorol 17:179–187

Liu Y, Linderholm HW, Song HM, Cai QF, Tian QH, Sun JY, Chen DL, Simelton E, Seftifen K, Tian H, Wang RR, Bao G, An ZS (2009) Temperature variations recorded in Pinus tabulaeformis tree rings from the southern and northern slopes of the central Qinling Mountains, central China. Boreas 38:285–291

Meko DM, Graybill DA (1995) Tree-ring reconstruction of upper Gila River discharge. Water Resour Bull 31:605–616

Mitchell TD, Jones PD (2005) An improved method of constructing a database of monthly climate observations and associated high-resolution grids. Int J Climatol 25:693–712

Pederson N, Cook ER, Jacoby G, Peteet DM, Griffin KL (2004) The influence of winter temperatures on the annual radial growth of six northern range margin tree species. Dendrochronologia 22:7–29

Shao XM, Fan JM (1999) Past climate on west Sichuan plateau as reconstruction from ring-widths of dragon spruce (in Chinese with English abstract). Quat Sci 1:81–89

Shi JF, Cook ER, Lu HY, Li JB, Wright WE, Sheng FL (2010) Tree-ring based winter temperature reconstruction for the lower reaches of the Yangtze River in southeast China. Clim Res 41:169–175

Sun JH, Zhao SX (2010) The impacts of multiscale weather systems on freezing rain and snowstorms over southern China. Weather Forecast 25:388–407

Wang ZY, Ding YH (2006) Climate change of the cold wave frequency of China in the last 53 years and the possible reasons (in Chinese with English abstract). Chin J Atmos Sci 30: 1068–1076

Wei FY (2008) The variation features of cold wave disaster under climate warming (in Chinese). Prog Nat Sci 18:289–295

Wen KG, Chen SX (2006) China meteorological calamity grand ceremony: Jiangxi volume (in Chinese). Meteorological Press, Beijing, pp 382–396

Wen KG, Ding YH (2008) China meteorological calamity grand ceremony: combined volume (in Chinese). Meteorological Press, Beijing, pp 474–518

Wen M, Yang S, Kumar A, Zhang PQ (2009) An analysis of the large-scale climate anomalies associated with the snowstorms affecting China in January 2008. Mon Weather Rev 137: 1111–1131

Wigley TML, Briffa KR, Jones PD (1984) On the average of value of correlated time series, with applications in dendroclimatology and hydrometeorology. J Clim Appl Meteorol 23:201–213

Yadav RR, Singh J (2002) Tree-ring-based spring temperature patterns over the past four centuries in western Himalaya. Quat Res 57:299–305

Yi MJ, Chen YJ, Zou RJ, Deng SM (2009) Analysis on isentropic potential vorticity for the snow calamity in Soutch China and the stratospheric polar vortex in 2008. Plateau Meteorol 28:880–888

Yonenobu H, Eckstein D (2006) Reconstruction of early spring temperature for central Japan from the tree-ring widths of Hinoki cypress and its verification by other proxy records. Geophys Res Lett 33:L10701. doi:10710.11029/12006GL026170

Zhang YM, Zhang PY, Gu X, Zhong J, Liu SH (2010) Analysis of climatic characteristics of cold wave in Guizhou Plateau (in Chinese with English abstract). Chin J Agrometeorol 31: 151–154

Zhao LN, Ma QY, Yang GM, Wang XR, Zhao LQ, Yang XD, Wu H, Wang Z, Kang ZM, Mao DY (2008) Disasters and its impact of a severe snow storm and freezing rain over southern china in January 2008 (in Chinese with English abstract). Clim Environ Res 13:556–566

Zhu QG, Lin JR, Shou SW, Tang DS (2000) Principles and methods in synoptic meteorology (in Chinese). China Meteorological Press, Beijing, pp 266–318

Zhu HF, Zheng YH, Shao XM, Liu XH, Xu Y, Liang EY (2008) Millennial temperature reconstruction based on tree-ring widths of Qilian juniper from Wulan, Qinghai Province. Chin Sci Bull 53:3914–3920

Zhu HF, Fang XQ, Shao XM, Yin ZY (2009) Tree ring-based February–April temperature reconstruction for Changbai Mountain in Northeast China and its implication for East Asian winter monsoon. Clim Past 5:1–6